J. Materials Conc. Struct., Pavements, JSCE, No. 564/V-35, 297-316, 1997 May

# NUMERICAL SIMULATION OF SIZE EFFECT IN SHEAR STRENGTH OF RC BEAMS

Xuehui AN[1], Koichi MAEKAWA[2] and Hajime OKAMURA[3]

[1] Member of JSCE, Dr. of Eng., Seismic Eng. Dept., Tokyo Electric Power Services Co., Ltd. (Higashi-Ueno 3-3-3, Taito-ku, Tokyo 110, Japan)
[2] Member of JSCE, Dr. of Eng., Professor, Dept. of Civil Eng., The University of Tokyo (Hongo 7-3-1, Bunkyo-ku, Tokyo 113, Japan)
[3] Fellow of JSCE, Dr. of Eng., Professor, Dept. of Civil Eng., The University of Tokyo (Hongo 7-3-1, Bunkyo-ku, Tokyo 113, Japan)

This paper presents numerical analysis on size effect in shear strength of RC beams, and its mechanism accompanying diagonal shear cracks is discussed. It is shown that the tensile stress transfer through bond mechanism and the strain-softening in both tension and shear associated with fracture energy are the main points which cause the size effect. A spatially averaged continuum constitutive model which covers the reinforcement-confined concrete and plain one is proposed for simulating unstable propagation of diagonal shear cracking. The model was verified by using the FEM program applied to RC beams in flexure and shear, and size effect experiments including RC of huge dimension were simulated.

***Key Words***: *size effect, shear strength, RC beam, FEM, fracture mechanics*

## 1. INTRODUCTION

The shear behavior of reinforced concrete members is an important topic of structural engineering research and a concern of engineers as the shear failure of concrete structures occurs suddenly, and lead to catastrophic failure. In order to capture the shear performance many efforts have been made in experimental and analytical studies. Numerous experimental results[1)-3)] have shown that the shear capacity of reinforced concrete beams without stirrup is significantly influenced by member size, that is, the nominal shear strength of a reinforced concrete member will be gradually reduced as the beam depth increases. This is called size effect on shear strength of reinforced concrete structures. In recent years, the scale of concrete structures has been becoming larger owing to the advances made in materials, design and construction technologies as well as scale-up economical performance of infrastructures such as energy facilities[5)]. The computation for these large scale reinforced concrete structures is also needed to investigate the size effect in shear strength. Development of this kind of numerical tools should be based on the correct understanding of the mechanism of size effect.

Size effect in shear strength of RC members has already been observed very clearly according to huge amount of experimental evidences. The experiment carried out on large reinforced concrete beams without shear reinforcement has examined that the size effect in shear strength exists in beams even when the depth reaches as large as 3 meters[4)]. There are some studies whose focus is addressed to design code on size effect[5)], and the numerical simulation was tried. Here exists a summary[6)] of the analysis on size effect experiment having the beam depth ranging from 10cm to 300cm. The analytically and experimentally obtained relationships between the applied load and the displacement at the center of the span of a specimen are shown in **Fig.1**.

Significant differences among each analysis method can been seen. The result predicted by A-analysis gives extremely higher stiffness as the tension softening is neglected. The stiffness predicted by some analysts tend to agree with the test result but the failure load is overestimated[7)]. One tendency in these computational results is that the predicted failure shows bending mode after the yielding of longitudinal reinforcing bars, but the reality is that the specimens failed in shear before the yield of main bars. The discussion on these analytical results makes it clear that the tension softening is an important factor for predicting the shear behavior of the RC members, especially the propagation of

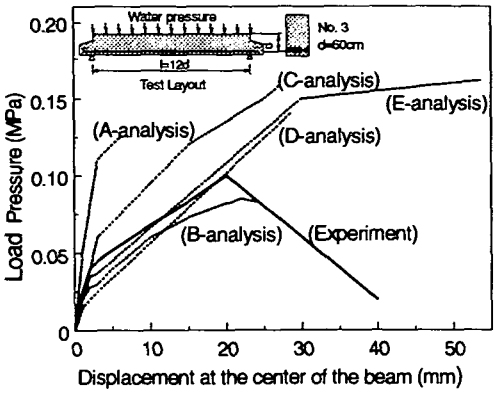


**Fig.1** Summary of analytical results on specimen No.3 [4),6)].

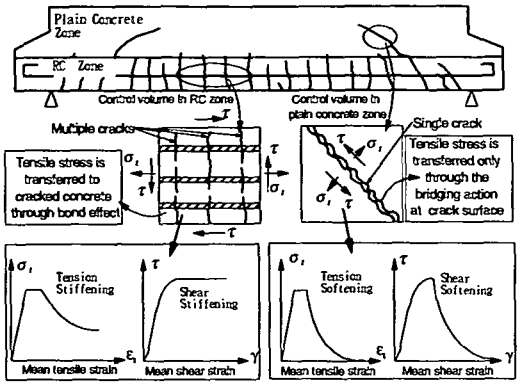


**Fig.2** Spatially averaged response defined on the control volume(element) of RC zone and plain concrete zone.

diagonal shear cracks. The factors which affect the failure mode and the capacity should be investigated.

In order to reproduce the size effect in numerical simulation and to predict the shear failure of RC members correctly, it is necessary to make clear what sources cause the size effect and how they affect the member behaviors. The mechanism of plain concrete size effect has been investigated in view of the fracture energy. By using the tension strain-softening model based on fracture energy requirement[11),13)], the size effect of plain concrete members is reported to be explained successfully. But, when we further challenge the size effect of RC, the existence of reinforcing bars and the concrete stress transferred by bond mechanism have to be considered. In this paper, these expected sources which influence the shear behavior of reinforced concrete members without shear reinforcement are examined in order to simulate the shear behavior of members with different sizes.

## 2. MECHANISM OF SIZE EFFECT

The size effect has been explained by several mechanisms such as the randomness of material strength causing the fact that in a larger structure it is more likely to encounter a material point of smaller strength[8)], or the aggregate interlocking action affecting the shear strength while the interlocking action is reduced as the member size increases[2)]. Later, the randomness of strength has been proved playing only a negligible role in most situations[9)] and the aggregate interlocking action becomes small as the depth of a beam is larger than 100cm[10)]. The size effect of concrete can be properly explained by the energy release caused by microcrack growth[11)], and the tension-softening characteristics of plain concrete is regarded as the core factor for the size effect of concrete members.

But for dealing with RC member as shown in **Fig.2**, the spatially averaged mechanical property of concrete near or far away from the reinforcement is supposed totally different as the concrete confined by steel bars will show stable stress release beyond cracks owing to the bond affecting either tension or shear. The concrete outside the bond effective zone is supposed the same as plain concrete, showing sharp strain-softening feature as the tensile stress is transferred only through the bridging action at the crack surface. In order to fully understand the mechanism of size effect of RC members, the other factors such as the bond effect of reinforcing bars and the shear softening of plain concrete should be investigated carefully, as these factors are thought to affect the shear behavior of RC members.

### (1) Tension softening of plain concrete

The fracture front blunting by the large size of microcracked zone has been raised[12),13)] as a form of fracture mechanism of concrete. The progressive microcracking in the fracture process zone may be described by a triaxial stress-strain relation that exhibits strain-softening with a gradual reduction of maximum principal stress to zero(**Fig.3**). The energy consumed per unit advance of the crack band, called the fracture energy, may then be expressed as[12)],

$$G_f = w_c \int \sigma_t d\varepsilon_t \qquad (1)$$

where, $\sigma_t$ ,$\varepsilon_t$ is the normal mean stress and mean strain defined in the crack; $G_f$ is the fracture energy and $w_c$ is the crack width.

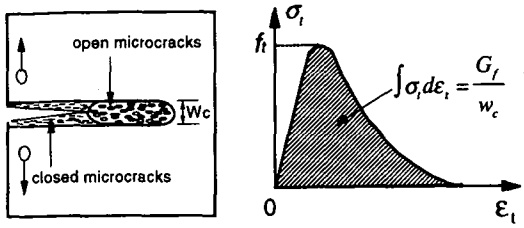


**Fig.3** Fracture process zone and tensile stress-strain diagram.

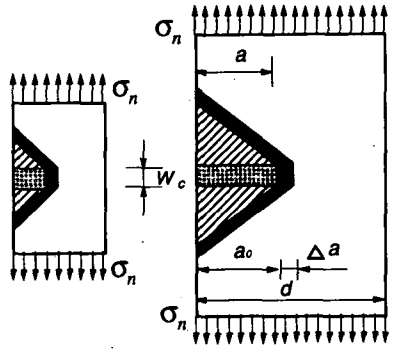


**Fig.4** Crack band propagation in member with different scale[13].

Here, to separate the size effect from other influencing factors, the geometrically similar concrete panels are studied as an example. Two panels of different sizes are assumed to have a weak spot in the middle of the left side, from which fracture originates (**Fig.4**). The fracture front may be considered in the form of a crack band of a certain width, an constant related to the material, independent of the structure size. Formation of a crack may be imagined to release stress and the initial strain energy of density from the cross-hatched area in **Fig.4**[12),13)]. When the fracture extends by a certain length, the initial strain energy that is released into the fracture front comes from the black strip of the horizontal dimension. It is instructive to note that in a larger structure the energy that is released to the fracture extension is larger if the load level is kept the same, because the energy is released from a larger zone. Therefore, the load level for a larger structure must be less so that the total energy release would remain the same. This is one of the size effect that nominal failure stress becomes smaller when the scale of the concrete structure becomes larger.

The numerical method for size effect simulation can be done by adjusting the strain-softening curve according the element size based on the fracture energy balance (**Fig.5**), as in the finite element computation, the crack width is replaced by element reference size. In this case, the cracked band is assumed localized in a element and adjacent ones are to be unloaded.

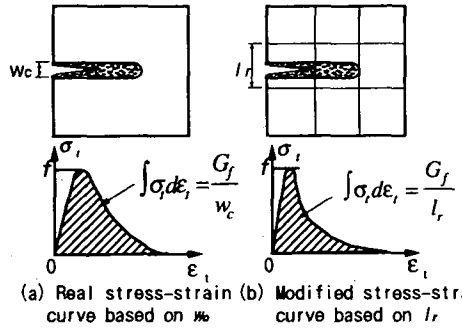


(a) Real stress-strain curve based on $w_c$ (b) Modified stress-strain curve based on $l_r$

**Fig.5** Tension softening model for FEM.

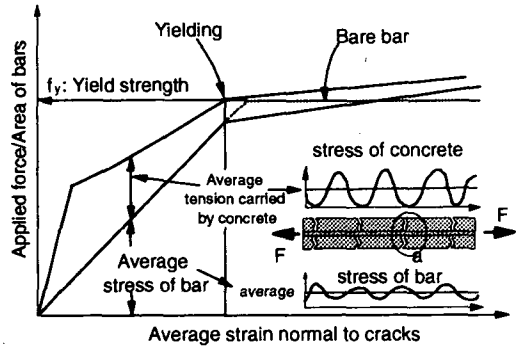


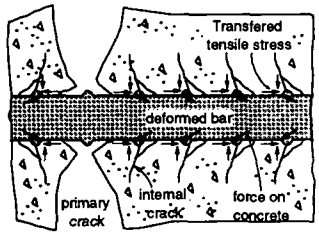


Micro mechanism of bond effect [15]

**Fig.6** Micro and macro aspect of bond and stress transfer.

### (2) Bond effect of reinforcing bars

The bond effect of reinforcing bars is thought to affect the overall characteristics of concrete surrounding steel bars (**Fig.6**). The bond between the reinforcing bars and concrete will enable some tension to be transferred from the bars to the concrete. This effect makes concrete capable of supporting a part of tensile force even after cracking has taken place in the reinforced concrete. **Fig.6** shows that even though the concrete ceases to support the tensile force at the crack section, the concrete continues to bear the part of the tensile stress transmitted from the reinforcing bars through the bond action. This makes the stiffness of the reinforced concrete remain higher than that of the reinforcing bars alone. The additional stiffness can be considered as coming from concrete. When the spatial average stress and the average strain relationship of concrete is constructed, it can be

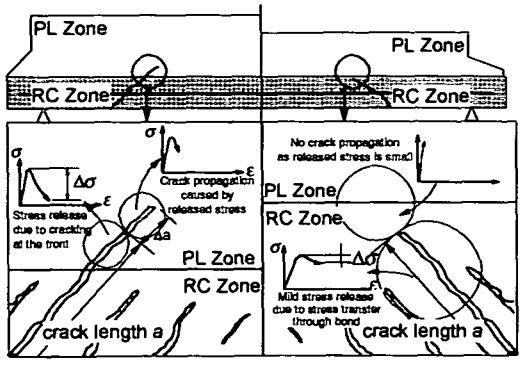


(a) Crack propagation.

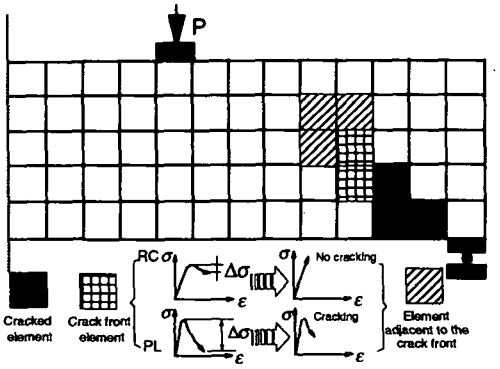


(b) Tension stress release in each zone.

**Fig.7** Tension-softening effect in FEM computation.

found out the concrete inside the bond affecting area will show gradual and stable stress release which is independent of the size of cracked concrete area unlike the sharp strain-softening popular to plain concrete[16), 30)].

The difference of concrete mechanics near or far from reinforcing bars should be taken into account by considering at least two different zones in RC members, one for the concrete near the steel bars, and showing tension-stiffening behavior (called as RC zone), and another one for the concrete outside the RC zone showing strain-softening behavior (called as PL zone). As the size of the RC zone is considered to be decided by the bond effect, which is related to the diameter and amount of the steel bar, and as the diameter of the steel bar will not always increase proportionally with the scale of the member, the size of the RC zone will not always increase proportionally with the scale of the member. Usually for a very large beam the ratio of bar diameter to depth of the beam is less than that of a smaller member, so the bigger beam will have a relatively smaller RC zone (**Fig.7a**).

Then, even though the geometrically similar propagation of cracking would be reproduced in both small and large beams, the crack front mechanical conditions with respect to the energy release are

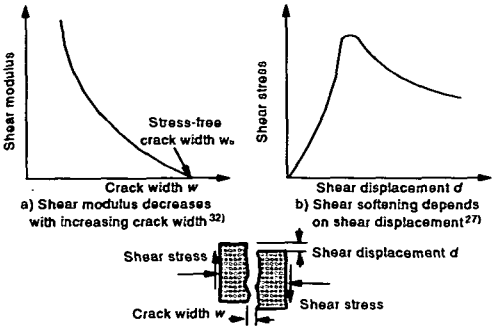


**Fig.8** Shear softening of plain concrete.

different due to non-proportional territory of plain and reinforced concrete. This non-proportionality can be one of sources of size effect, too.

As the concrete in RC and PL zones has different behaviors on mean tension stress-strain relation, once the cracks propagate into a finite element, the normal stress release will be much higher if this element is in the PL zone. In this case, the neighborhood elements are more easily cracked owing to the higher normal stress releasing (See **Fig.7b**). On the contrary, when the crack front would remain in RC zone, small tensile stress release due to mild softening would provoke less nonlinearity in adjoining elements. So in the computation, the cracks in RC member with relatively smaller RC zone may develop rapidly (**Fig.7b**).

### (3) Shear softening of plain concrete

For concrete surrounding reinforcing bars, the shear stiffening characteristics along cracks was observed when analyzing the mean behavior of concrete in shear and steel bars[5)]. Then, element-size sensitivity to the shear stiffness is neglected. But for plain concrete, it will lose shear transfer capacity and exhibits the softening and fracturing. In some researches[32)], this shear softening is obtained by decreasing the shear stiffness as a function of the strain normal to crack (**Fig.8a**). This is based on the fact that the interlock of aggregate particles diminishes with increasing crack opening. The studies on mechanism of stress transfer across cracks in concrete[27),28),29)] show the shear softening is also a function of shear displacement along the crack (**Fig.8b**). The unstable shear failure can only be simulated with understanding of shear softening based on normal and shear displacements. As the same story on tension softening, the energy release rate when the shear crack is developing will be approximately constant with a lower load level for larger structure. Therefore, in a larger concrete structure, the shear crack may propagate quickly than

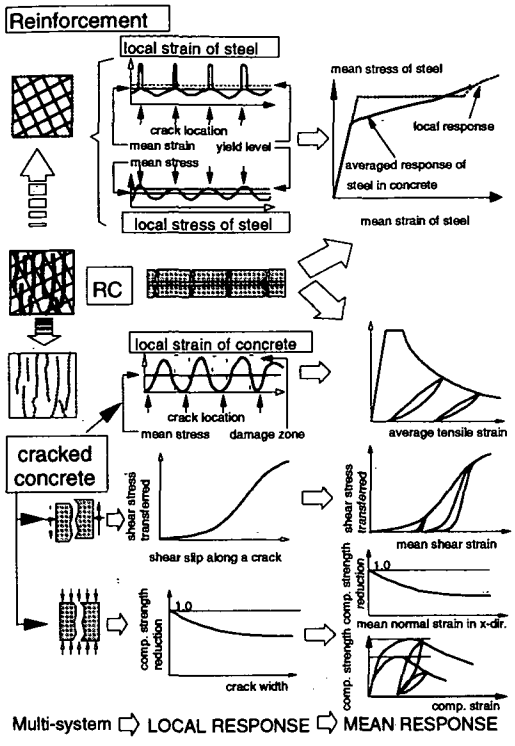


**Fig.9** Cracked concrete model for conecrete in RC zone[5].

the smaller one and the unstable shear crack may occur more suddenly.

## 3. PROPOSED MODEL FOR CONCRETE IN RC ZONE AND PL ZONE

Constitutive models are proposed to simulate shear size effect by finite element method for engineering purpose. The smeared model is used for cracked concrete with the fixed multi-directional cracks and all the stress-strain relationships are based on the spatial average stress and average strain of concrete defined in finite elements. Here, the consistency in terms of fracture energy in mode I is discussed.

### (1) Cracked concrete model in RC zone[16]

The reinforced concrete model has been constructed by combining the constitutive law for concrete and that for reinforcing bars (**Fig.9**). The constitutive law adopted for the cracked concrete consists of the tension stiffening model, the compression model and the shear transfer model.

Once cracks are generated in the concrete, the anisotropy becomes significant so that the stress-strain relationship takes on an orthogonal anisotropy along crack direction. The stress-strain relations can be modeled respectively in the directions parallel as well as normal to cracks and in the shear direction.

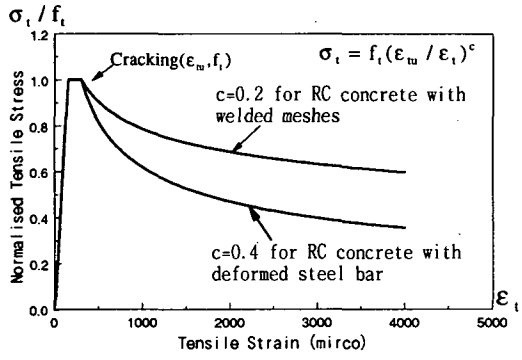


**Fig.10** Tension stiffening model for concrete in RC zone[16].

Owing to bond of concrete to the reinforcing bars, the concrete continues to support a part of the tensile force even after cracking has taken place and been distributed in a reinforced concrete, as mentioned in the previous section. In order to consider the influence of bond effects, the relation between the average stress and average strain of concrete is given as the tension model for cracked concrete. This tension model shows tension stiffening because of taking account of the stress transferred from steel bars by bond effect.

The tensile model of cracked concrete with tension stiffening can be described as the following[16] (see **Fig.10**).

$$\sigma_t = \sigma_t(\varepsilon_t; c) = f_t\left(\frac{\varepsilon_{tu}}{\varepsilon_t}\right)^c \qquad (2)$$

where, $\sigma_t$ : mean tensile stress normal to cracks, $f_t$ : tensile strength of concrete, $\varepsilon_t$ :tensile strain normal to cracks, $\varepsilon_{tu}$ :cracking strain of concrete, $c$: stiffening factor.

Different bond characteristics can be modeled by changing the sharpness of the tension-stiffening curve. For example, the constant $c$ which describes the sharpness of the stress release can be set 0.4 for ordinary deformed bars and 0.2 for welded wire meshes [16].

This constitutive law for reinforced concrete derived for a control volume of 30-50 cm sized concrete element with distributed cracks is independent of crack density and crack numbers owing to the trade-off mechanisms among these effects[30]. It is proved that in the case of normal concrete and two-way reinforcement with the ratio over 0.1% up to 2%, this two dimensional constitutive law is independent of the size of the control volume. This cracked concrete model is rather simple as the mean behavior of the cracked concrete is unrelated to the spacing of cracks, the direction of reinforcing bars and the reinforcement ratio without any size sensitivity[30]. Cracks do not

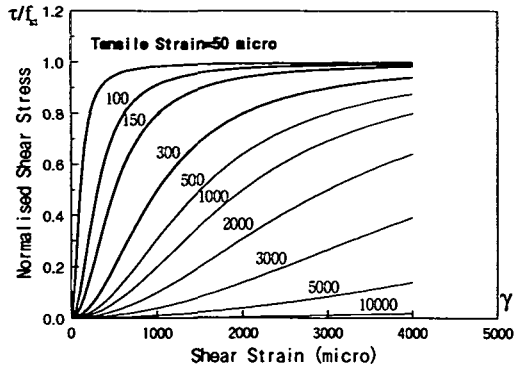


**Fig.11** Shear stiffening model for concrete in RC zone[16].

appear even just after the stress generated has attained its cracking stress, but there is a certain amount of plastic deformation. This has been expressed in the present model by assigning the tensile cracking strain that is twice as much as the tensile strain for the tensile strength of concrete[17].

The shear model of cracked concrete in RC is based on the contact density idealization[18] and ignores the elastic component in the deformation at contact crack plane. The model gives the shear stress in terms solely of the shear slip to crack width as,

$$\tau = G \cdot \gamma \tag{3}$$

where, $\tau$ : mean shear stress, $\gamma$ : mean shear strain, $G$ : secant shear modulus as,

$$G = \frac{1}{1/G_{st} + 1/G_c}$$

$G_c$ : shear modulus of uncracked concrete, $G_{st}$ : intrinsic shear modulus due to cracks as,

$$G_{st} = \frac{\tau_{st}}{\gamma} = f_{st}\frac{\beta^2}{1+\beta^2},\quad \beta = \frac{\gamma}{\varepsilon_t}$$

$\varepsilon_t$ : tensile strain normal to crack plane, $f_{st}$ : intrinsic shear strength ( $f_{st} = 18 \cdot f_c'^{1/3}$ :kgf/cm$^2$ ) [24].

In this model, the shear stress is normalized by the intrinsic shear strength as shown in **Fig.11**. It was mathematically and experimentally proved that the shear stiffness of cracked concrete zone is not affected by the crack spacing and density[18]. It means element-size insensitivity of shear behavior along cracks in RC zone.

### (2) Effective size of RC zone

The effective size of RC zone will be an very important factor for size effect computation. Different size of RC zone in an analysis domain may have effect not only on the stiffness of member after cracking, but also the failure mode which will be

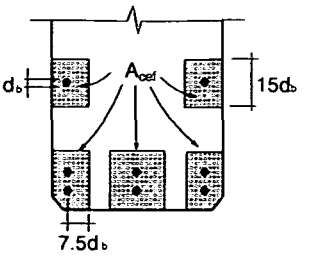


**Fig.12** Example of the definition of RC zone[14].

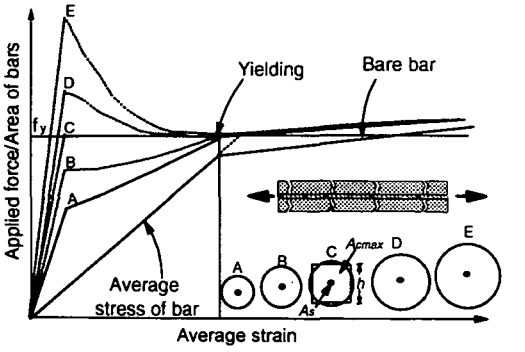


**Fig.13** Crack control capability and concrete area.

changed from shear to bending as the size of RC zone increases. The effect of RC zone will be verified later in this paper.

The size of RC effective zone is related to the bond effect of reinforcing bars and should be decided by the bond characteristics. There are many researches about the bond strength and bond-slip relation between steel bar and surrounding concrete, and the area of effective embedment zone of concrete is given as a function of steel bar diameter. **Fig.12** gives an example of the definition of the effective embedment zone for computing the crack width of RC flexural members[14].

When the area of the concrete surrounding a certain steel bar is becoming larger, the steel bar yields earlier after a crack is formed. Here much stress carried by concrete will be transferred to the steel bar (**Fig.13**). In one critical case, if a reinforced concrete member that is subjected to tension contains only a very small amount of reinforcement, the reinforcement crossing the crack yields just after cracking and most deformation will be rooted in this single crack. This is a critical point whether the adequate crack control capability with several cracks can be obtained or not.

When the first crack occurs, tension must be transferred from concrete to the reinforcement, resulting in an increase in steel stress at the crack section. If the area of concrete is too large, the stress increase will be about equal to the yield strength of reinforcement. Hence, for one certain steel bar, the

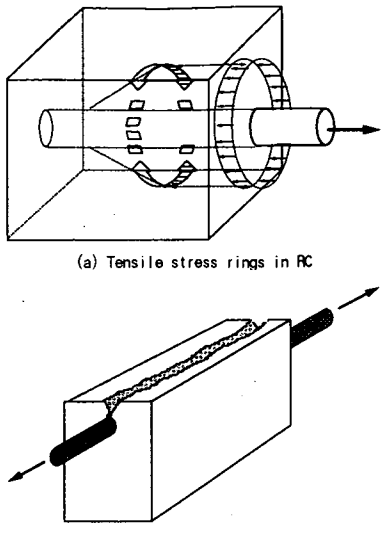


**Fig.14** Cover concrete failure[19].

maximum size of concrete zone where several cracks can develop is,

$$A_{cmax} = \frac{A_s \cdot f_y}{f_t} \tag{4}$$

where, $A_s$ : cross-sectional area of steel bar, $A_{cmax}$ :maximum area of bond effective zone in concrete, $f_y$ : yield strength of steel bar.

In two dimensional computation, it is more convenient to use the relation between RC zone height as shown in **Fig.13** and steel bar diameter as,

$$h_{max} = \frac{\sqrt{\pi}}{2} \cdot d_b \cdot \sqrt{\frac{f_y}{f_t}} \tag{5}$$

where, $h_{max}$ : the height of RC zone, $A_{cmax} = h_{max}^2$, $d_b$ : diameter of reinforcing bar.

The height of RC zone calculated by Eq.(5) indicates the maximum size of RC zone. The height used in computation may be smaller than this value according to the arrangement of steel bars.

The formula above shows the RC zone size when the cover concrete is thick enough to provide the sufficient bond effect. There is a tensile stress ring in the concrete which balances the concrete radial components of inclined compressive strut forces (**Fig.14a**)[19]. If the cover concrete is not thick enough, the ability of a deformed bar to transfer its load into the surrounding concrete is typically limited by the failure of this tension when the concrete cover is splitted (**Fig.14b**).

In this case, the ultimate local bond strength is governed by the resisting capacity against entire

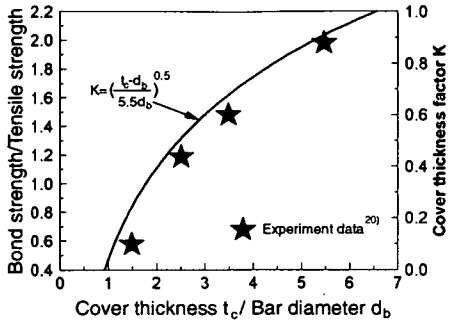


**Fig.15** Cover effect on bond strength and factor *K*.

splitting of the concrete cover. The experimental studies to confirm the cover effects in the longitudinal splitting crack formation were conducted.[20),21)] Some results of the relation between bond strength and the specific cover are shown in **Fig.15**. The bond strength decreases as the concrete cover decreases. So in the case of insufficient cover, the formula in Eq.(5) should be factored by $K$, which is a empirical function based on test result[21)] as,

$$K = \left( \frac{t_c - d_b}{5.5 d_b} \right)^{0.5} \tag{6}$$

where, $K$ : cover thickness effect factor, $K$=0 when $t_c < d_b$ and $K$=1 when $t_c > 6.5 d_b$, $t_c$ : the thickness of the concrete cover.

In the two dimensional finite element computation, it is needed to decide the height of RC zone including steel bars with different kinds of arrangement. The basic rule is that the height of RC zone is decided by the diameter of each bar. If a bigger bar is used, the RC zone is larger (**Fig.16a**). In the case where more than one layer of steel bars are used, the RC zone should be calculated according to each layer.

When RC zones overlap with each other due to dense arrangement of bars, the overlapped area is simply treated as a part of RC zone in principle. No double account of area is made since tension stiffness of cracked concrete in RC is found independent on the reinforcement ratio [30)].

Another extreme case is that the steel bars are placed away from each other. In this case, the size of RC zone may be smaller than the one computed from Eq.(5), as the steel bar can not control the crack distribution in the whole volume of concrete in the section (**Fig.16b**). The hight of RC zone used in computation is hereafter proposed as,

$$h_e = \frac{n \cdot h_{max}^2}{b} \tag{7}$$

where, $h_e$ : modified height of RC zone, $n$ : number of steel bars, $b$ : thickness of RC member.

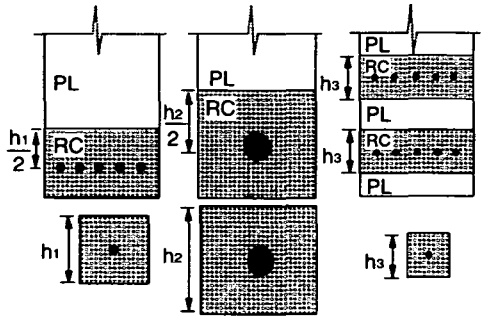


(a) $h_n \le h_{max}$

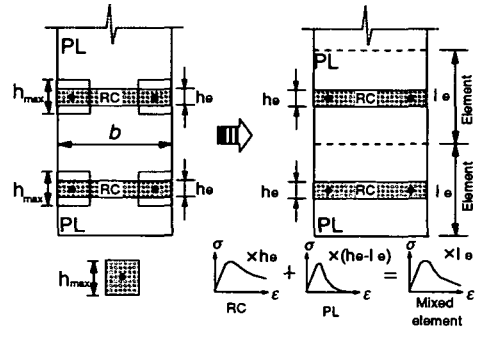


(b) Bars with large distance ( $h_e < h_{max}$ )

**Fig.16** RC zoneing method.

When the bars are very small or far away from each other, the modified height of RC zone will be too small for finite element discretization. It is needed to consider the situtation that one element contains both RC and PL zones. The stress-strain curve of this element with mixed zones can be decided by solving the coefficient $c_m$ from the following equation of fracture energy balance as,

$$\int_0^{\infty} \sigma_t(\varepsilon_t; c_m)d\varepsilon_t = \frac{(l_e - h_e)\int_0^{\infty}\sigma_{PL}d\varepsilon_t + h_e\int_0^{\infty}\sigma_{RC}d\varepsilon_t}{l_e} \quad (8)$$

where, $\sigma_{RC} = \sigma_t(\varepsilon_t; 0.4 or 0.2)$ as defined in section 3 (1). $\sigma_{PL} = \sigma_t(\varepsilon_t; c_{pl})$ where $c_{pl}$ will be defined later, $l_e$: height of the finite element.

### (3) Cracked concrete model in PL zone

As discussed above, the cracked plain concrete shows strain-softening characteristic in tension and shear comparing with the concrete confined by reinforcing bars. The stress-strain curve is decided with respect to the fracture energy and the crack band width[12]. The crack band width in computation becomes the reference length related to the element size. The fracture energy is treated as a material property and needed to be kept constant regardless of the element size. Some typical shapes of tension

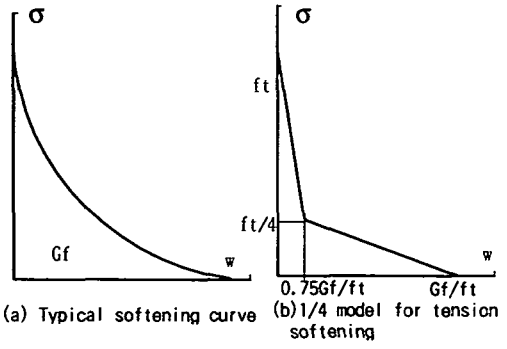


**Fig.17** Tension softening curve for plain concrete[22].

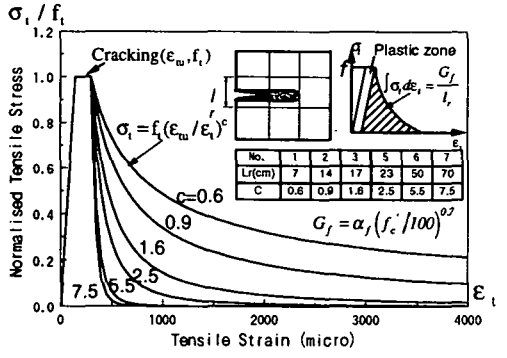


**Fig.18** Tension stress-strain softening curve in computation.

softening curve[22] are shown in **Fig.17**. Based on the fracture energy balance, the stress-strain curve defined in a element needs to be modified according to the element geometry. Within the scheme of smeared crack approach, total fracture energy performed in an element is equal to the product of element volume and the specific fracture energy (shaded area in **Fig.18**) associated with the averaged stress-strain relation. As tensile fracture is highly anisotropic, consumed fracture energy and the reference length as shown in **Fig.5** are related to the direction of crack propagation and the element geometry.

As a matter of fact, crack propagating directions may be arbitrary in the analysis of RC beams with flexural as well as diagonal shear cracking. But, in the case of circular elements, the length is constant regardless of the crack orientation. Then, the authors provisionally adopt the square root of the element area as an averaged referential length. The validity of this assumption for beam analysis case will be checked with different shapes and sizes of elements in later section. The rationality of this assumption should be examined in future for other engineering problems ($l_r$ is defined as the square root of the element area).

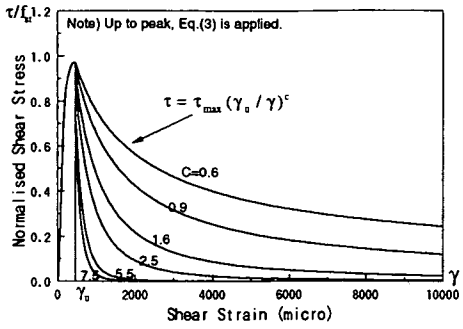


**Fig.19a** Shear stress-strain softening curve for plain concrete. (tensile strain =0.00005, ultimate shear strain $\gamma_u$=0.0004 )

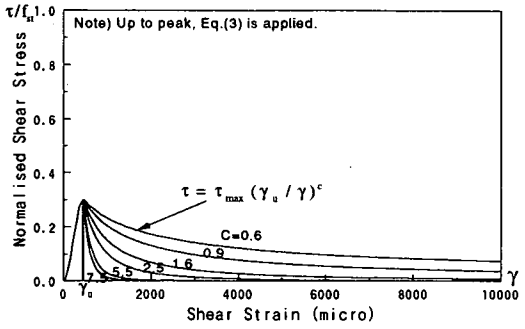


**Fig.19b** Shear stress-strain softening curve for plain concrete. (tensile strain =0.0005, ultimate shear strain $\gamma_u$=0.0004)

There are several ways to decide the shape of tensile stress-strain curve which satisfies the coherency of the fracture energy. The plastic zone of the applied tension model in Eq.(2) was decided so that the capacity of plain concrete beams in flexure can be simply obtained.[16),34)] The following descending portion may influence the load bearing of plain concrete. In this analysis, however, softening curve under the higher straining of element was found not to be sensitive to the shear capacity of RC beams, because bending cracks in which larger opening strains may occur is mostly included in RC zones with coupled high stiffness of reinforcement. In the proposed model of the authors, the same functional formula with the tension model of cracked concrete in RC zone is used for simplicity and consistency in computation. The stiffening factor will change with the element size by getting the constant fracture energy. **Fig.18** gives a series of tensile stress-strain curves for the computation of beams with depth varying from 10cm to 300cm which will be used in size effect analysis in later section.

In this study, the tensile fracture energy used in analysis was specified by using CEB-FIP model code (1990) equation written in **Fig.18**. For deciding the aggregate size related factor $\alpha_f$, Wittmann's test[35)] was referred.

In the process of diagonal shear failure of RC members, shear mode fracturing model along a propagating crack band is thought to be influential. Lim, et al. reported[36)] that the sliding shear fracture energy in softening region is consumed partly in terms of plastic frictional mode dependent on the normal confinement and, to some extent, absorbed by the damaging of shear band which accompanies the unrecoverable reduction of stiffness. Bujadham et al. proposed an enhanced contact density model[36)] for a single crack stress transfer which is derived from a coupled fracturing and plasticity at contact planes of two crack faces.

These researches signify that shear fracture energy of plain concrete is not unique unlike the tensile fracture of crack band, but highly dependent on the crack opening or normal confinement like stable cracks in reinforced concrete[30)]. At the same time, the averaged shear stress-strain relation along a crack band has to be adjusted by the element size and shapes in terms of shear fracture energy. Because, the shear fracturing is also localized and coupled with mode-I tensile fracture. The shear fracture model of plain concrete band is a mixed mode feature and to be governed by both the crack opening, similar to the stress transfer model for RC, and an element size as is the case of tensile fracture model for PL zone.

In this study, a simple shear fracturing model which satisfies the above requirement for plain concrete is employed by combining the stress transfer model for cracks in RC zone and the energy balance requirement in shear as shown in **Fig.19**. In the ascending portion, Eq.(3) can be applied. When the shear strain exceeds the ultimate shear limit, softening branch is assumed. Regarding the shear softening rate is concerned, Lim et al. reported the experimental data and damage modeling under the constant compressive confinement[36)].

But, data is hardly available for mixed shear fracturing and crack opening except for Bujadham's experiment, which may be actualized in the shear failure of reinforced concrete. Then, the authors provisionally assume the same rate of softening as that of the tension fracture. The assumed shear fracture modeling of simplicity regarded as a rough equivalence to Bujadham's proposal and its contribution to the shear capacity of members will be examined through the sensitivity analysis in later chapter. On this matter, further investigation is strongly recommended.

Now, the proposed model for shear behavior can be summarized as the combination of cracked concrete model in RC zone and PL zone, based on the RC zoning method. In the FEM computation, the whole

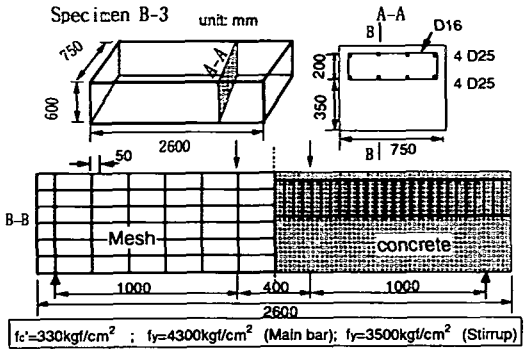


**Fig.20** Experimental layout.

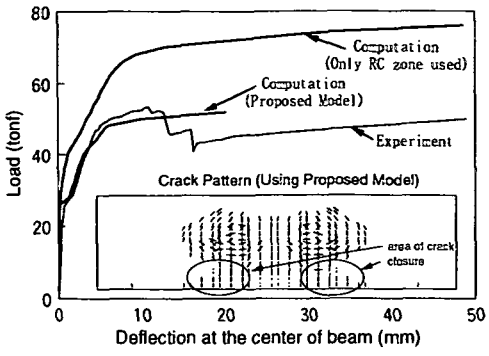


**(a)** Crack pattern and computed deflection

**(b)** Photo of the specimem after failure.

**Fig. 21** Bending behavior prediction for zoning check test.

RC member is divided into both RC and PL zones. In each zone the suitable strain-stiffening or strain-softening model is to be adopted.

## 4. VERIFICATION OF PROPOSED MODEL

Shear failure of RC beams is simulated in use of the proposed computational model. And the flexural response is checked for specially designed beam for experimental verification of the RC/PL zoning method proposed in the previous chapter. In this study, FEM program **WCOMR**[17] including the concrete model proposed was used for verification.

### (1) Flexure of RC beams

In order to check the definition of the size of RC zone proposed in Chapter 3, a specially designed beam was made. The beam was reinforced only in the top half and the rest half part in the bottom was kept as plain concrete (**Fig.20**). The beam was designed so that it fails in bending mode and diagonal shear failure is prevented by heavily arranging the web reinforcement.

In the computation, computed yielding load is much elevated and far away from the reality if the model for concrete in RC zone is applied to the entire volume of the specimen. **Fig.21a** shows the comparison of the test and the computational results which derive from the proposed model on zoning method. The yield load is correctly predicted in the finite element computation. The specimen shows very good ductility after yielding of longitudinal reinforcing bars and the crush of concrete in the top extreme fiber. This ductility comes from the good confinement by heavily reinforced web bars. For ductility, 3D computation is indispensable and will be reported in future.

The crack pattern obtained by the computation is shown in **Fig.21a**. A crack line does not indicate a point-wise information, but it represents the blunt area which Gauss integration point in an element numerically covers. As 2nd-order quadrilateral isoparametric elements with 3x3 integration points are used as shown in **Fig.20**, 9 crack lines can be drawn inside when a RC element is under tension nonlinearity such as bending cracking zones. Here, crack spacing is not computed and in fact, not necessary for mechanical simulation of RC domains. Of course, the graphical spacing of adjacent crack lines does not make any information. It has to be noted in smeared crack approach that the graphical image of crack patters does not coincide with the geometrical reality, but indicates the blunt information of stress release rooted in cracking, and mechanically sharp localization in a PL element is implicitly taken into account in energy balance consistency as discussed in Chapter 3.

In comparison with **Fig.21b** with the consideration above, coincidence of cracking is seen. The vertical cracks developed very rapidly up to the middle part of the specimen and then, the horizational cracks occured along the longitudinal bars.

The width of crack lines is drawn proportional to the strain normal to cracking. The cracks in the bottom part idealized by PL zones are less dispersed. A few vertical crack lines are thick, but adjacent crack lines are thin because the crack strain was oppositely decreased after the crack occurrence. This means localization of cracking fracture in PL zone.

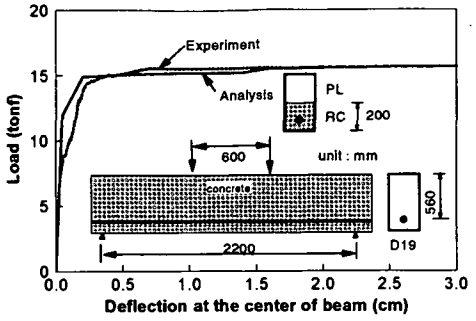


**Fig.22** Load-deflection relation of RC beam[24].

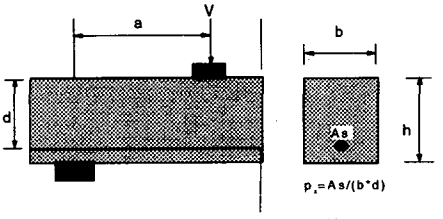


**Fig.23** Layout of the tests[1,33].

One more computation has been done for the prediction of imported bending test[24]. The experimental layout is shown in **Fig.22**. This test was done for beams with low reinforcement ratio, and steel bars are only in the lower part of the specimen. The upper part shows the behavior of plain concrete. The computational and experimental results are shown in **Fig.22**.

The verification of the RC/PL zoning method will be also checked in terms of shear failure in the next section.

### (2) Shear experiment of RC beams

In order to confirm that the proposed model may predict the shear behavior of RC members, some experiments of beams in shear were used as a target of interest. Not only the shear capacity but also the crack propogation will be checked to make sure that the program can simulate the unstable crack propagation of diagonal shear cracks.

The first series of beams in shear includes 5 beams which failed in shear mode[1),33)]. Beam No.1,2,3 were tested by Leonhardt and Beam No.4,5 were tested by Kani. The depth of the beam varied from 7cm to 109.5 cm. **Fig.23** and **Table 1** show the layout and data of the experiment. The computational and experimental ultimate loads are compared in **Table 1**. First, it can be seen that the use of the proposed cracked concrete model brings about the correct shear strength.

In **Fig.24** the computed cracking pattern is shown to clarify the failure mode. **Fig.24a** gives the crack pattern at the load step just before failure. In this

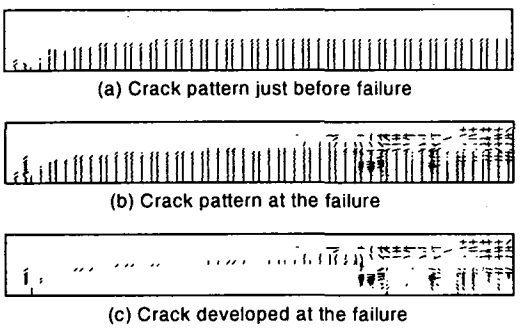


**Fig.24** Computed crack pattern of test No.5.

**Table 1** Dimension and shear capacity of the tests.

| | a/d | d | $p_x$ | $V_{u1}$ | $V_{u2}$ | $V_{u2}/V_{u1}$ |
|---|---|---|---|---|---|---|
| | | cm | % | tonf | tonf | |
| 1 | 3 | 7 | 1.71 | 0.74 | 0.66 | 0.89 |
| 2 | 5.8 | 27.8 | 2.00 | 6.7 | 5.50 | 0.82 |
| 3 | 3 | 45 | 1.33 | 10.35 | 11.9 | 1.15 |
| 4 | 6.8 | 55.6 | 2.72 | 8.53 | 8.36 | 0.98 |
| 5 | 8.7 | 109.5 | 2.68 | 15.0 | 14.8 | 0.99 |

Note: $p_x$ : reinforcement ratio; $V_{u1}$ : tested ultimate shear load; $V_{u2}$ : computed untimate shear load .

figure, just bending cracks can be seen. **Fig.24b** gives the crack pattern at the failure step. It can be seen that in the final step, some cracks developed suddenly in the middle and upper parts of the beam near the load point. These new developed cracks are inclined ones typical to shear failure. In order to see more clearly where the failure takes place, only the cracks which developed in the last step are drawn in **Fig.24c.** The additional cracking of the final step at the iterative process, that is associated with the unstable equilibrium under constantly fixed applied load, is thought to be a sequential trace of crack propagation in a blunt but localized area. The suddenly developed inclined shear cracks which cause the failure of this beam can be observed.

Another series of experiment for shear behavior is taken from Ref.25, which reports two beams without stirrups. One of the beam has longitudial reinforcement only near the top and bottom faces, while the other has longitudial reinforcement distributed over the height of the beam (**Fig.25**).

The experimental result on ultimate shear force is 200kN, for the case with reinforcement only near the top and bottom faces and for the one with distrubted bars, is 312kN. It can be seen clearly that the reinforcement in the centeral part increases the shear capacity so much as the concrete in the central part can fairly transfer tension owing to the reinforcement. This is also an evdience that how much tension and shear softening of plain concrete affect the shear behvaior of RC members. In computation, the ultimate load for these two cases are 196kN and

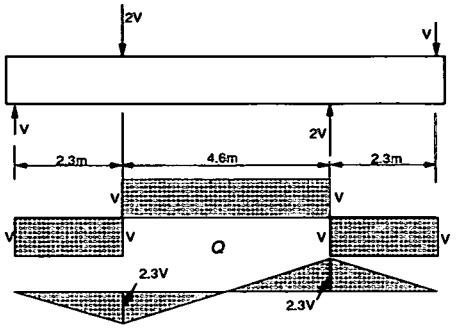


(a) Loading set-up .

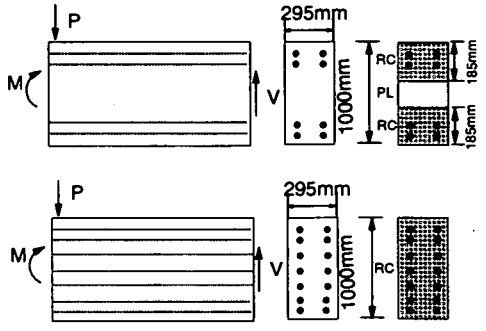


(b) Reinforcement layout

**Fig. 25** Targeted shear beams[25] for verification.

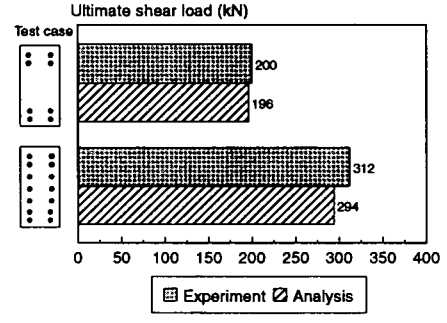


**Fig.26** Shear capacity comparision.

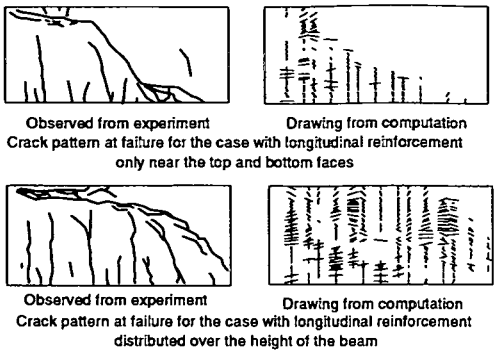


**Fig.27** Crack pattern comparision.

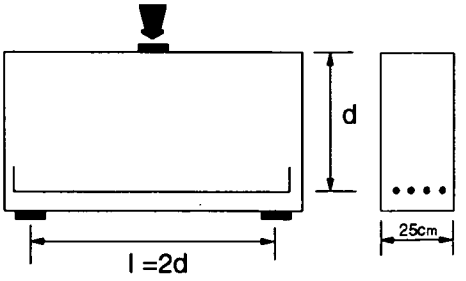


**Fig.28** Layout of shear test on short beams.

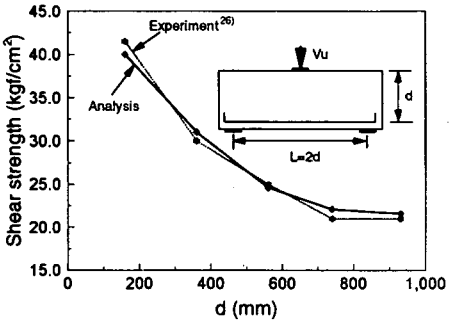


**Fig.29** Nominal shear strength of short beams with different size.

294kN. They are close to experimental results (see **Fig.26**).

The crack pattern comparision of these tests is shown in **Fig.27**. The existence of reinforcing bars in the middle part of the beam is capable of controling cracks and the computation can follow this difference of crack pattern reasonably.

### (3) Varying size experiment on shear strength of RC beams

Here two series of size effect tests on shear strength of RC beams without shear reinforcement are used. One is deep beam with depth from 16cm to 96cm, and the other is the beam with depth varying from 10cm to 300cm. The experimental layout and dimension of the deep beams[26] are shown in **Fig.28**. The common mixture of concrete was used for these different sized short beams. The maximum coarse aggregate size was 16 mm. In all the tests the slenderness ratio was equal to 1:1. The reinforcement ratio was approximately 1.1% so that they are all over-reinforced in bending. The thickness of all the specimen was 25 cm. The depth of these beams are 16cm, 36cm, 56cm, 74cm and 93cm.

In **Fig.29** the shear strength of these beams is represented as a function of the effective member depth. It is shown that the ultimate bearing capacity has a strong size dependence.

**Fig.30** shows the observed and computed cracking patterns of beam No.1 and No.5, at the same load step when the nominal shear stress value is 20kgf/cm$^2$. The difference of crack propagating level is very clear, where at this norminal shear stress the small beam remains in an early stage of flexural cracking.

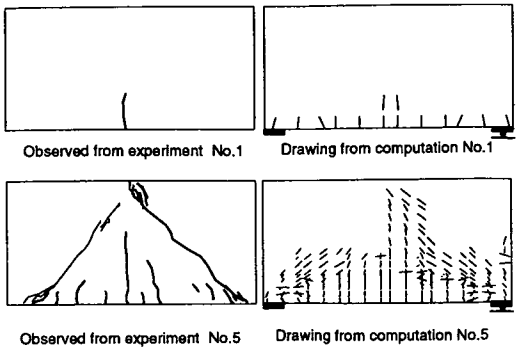


**Fig.30** Cracking patterns in short beams at the same nominal shear stress (20kgf/cm$^2$).

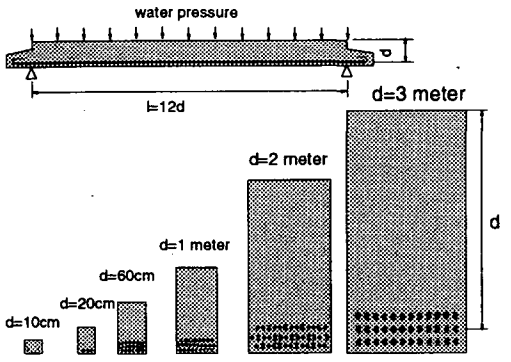


**Fig.31** Details of the cross section and arrangement of reinforcing bars[4].

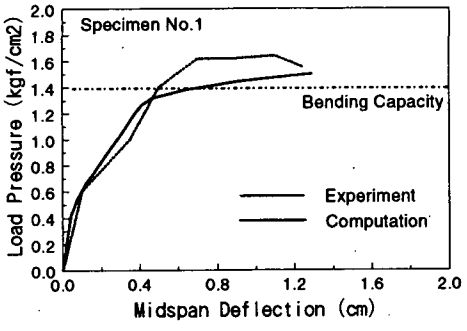


(a) No.1.

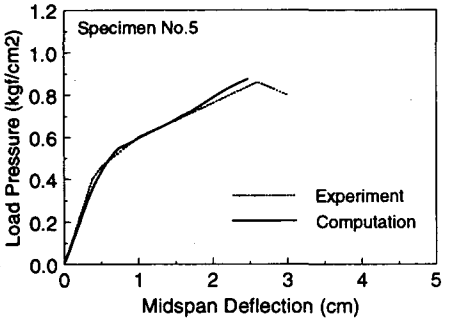


(d) No.5.

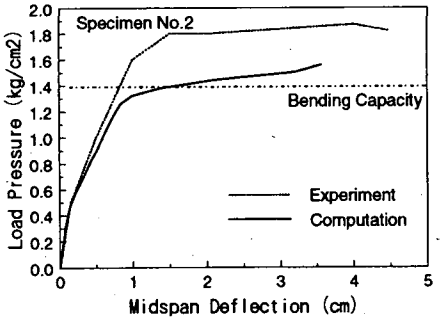


(b) No.2.

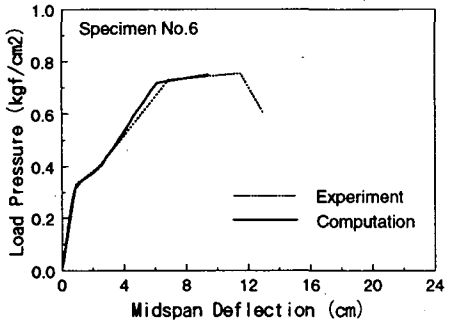


(e) No.6.

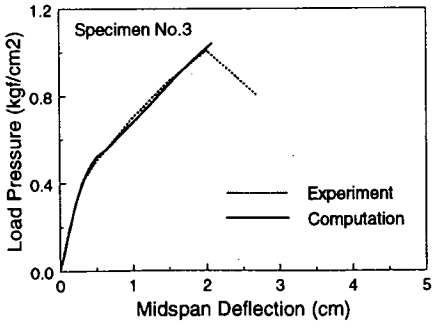


(c) No.3.

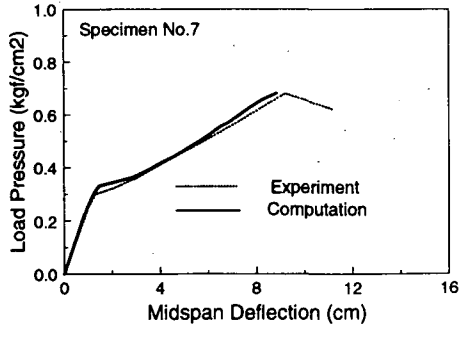


(f) No.7.

**Fig.32** Load-deflection relation at midspan for specimens.

Table 2 Specified properties of RC beams[4].

| | Depth | Concrete strength | Shear Strength | Shear Strength |
|---|---|---|---|---|
| | d | $f_c'$ | Exp. | Comp. |
| | cm | kgf/cm$^2$ | kgf/cm$^2$ | kgf/cm$^2$ |
| 1 | 10 | 202 | (7.38) | (6.75) |
| 2 | 20 | 193 | (8.41) | (7.02) |
| 3 | 60 | 207 | 4.55 | 4.59 |
| 5 | 100 | 215 | 3.87 | 4.05 |
| 6 | 200 | 279 | 3.40 | 3.51 |
| 7 | 300 | 240 | 3.09 | 3.24 |

But the large beam has already failed. It can be seen that the path-dependent analysis can simulate this size effect in crack propagation. In computation, no compressive softening occurs, but the unstable propagation of diagonal cracking rules failure of the short beams used in the analysis.

The other series of size effect experiment is for large RC beams[4] without shear reinforcement having different effective depth, 10cm, 20cm, 60cm, 100cm, 200cm and 300cm as shown in **Fig.31**. The ratio of loading span to effective depth is 12. The specified properties are listed in **Table 2**. The main reinforcement ratio in the vicinity of support points where shear failure would occur is taken to be 0.4%. The beams were loaded by uniformly distributed hydraulic pressure until failure. The observed failure modes were flexural failure for beam No.1 and No.2 and the shear failure for the other beams left.

The reinforced concrete beams without shear reinforcement was analyzed using the same program **WCOMR**, in which the discussed models are adopted. **Fig.32** shows the load-deflection relation for analytical and experimental results of specimen No.1-No.6.

It can be seen that, for specimen No.3, No.4, No.5 and No.7 the analytical results are close to the experimental ones. But for specimen No.1 and No.2, the computed capacity is lower than the experiment. In fact, the tested capacity for these two small beams is much higher than the bending capacity which is computed by RC beam theory of plane cross section. It is guessed that the loading membrane made of rubber would act as fiber resistant component attracted to the extreme top fiber of concrete. As for the small beam with depth less than 20cm, the stiffness of 1-2cm thick rubber might not be neglected.

**Fig.33a** shows the crack pattern of specimen No.3. The short lines in the computed crack pattern picture are not associated with individual discrete cracks. They represent the smeared cracks, whereas the thickness of line indicates the magnitude of normal strain corresponding to the opening of cracks, and from the direction of the lines crack orientation

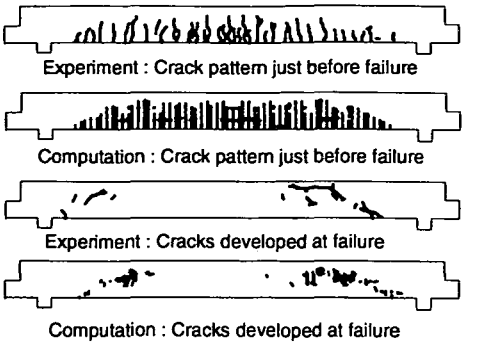


**Fig.33a** Crack patterns for specimen No.3.

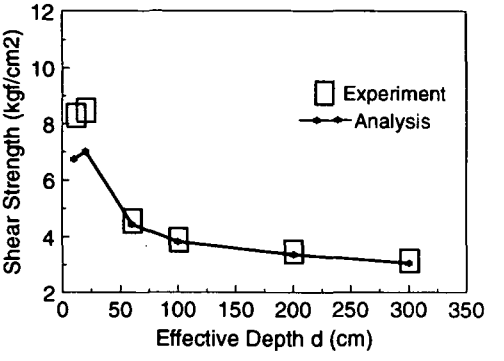


**Fig.33b** Size effect comparison.

can be distinguished. It can be seen that the computation exhibits the shear cracks almost at the same place as the experiment and the crack opening is larger near the right side of support. In both analysis and experiment, transitional displacement at the right support is specified as being free and the left one is fixed. In any case of computation, diagonal shear failure takes place at the side having the roller support (See **Fig.30**) owing to stationary energy release. In order to confirm the failure mode and location, as introduced above, the cracks which developed at the final step is also shown in the figure. It shows that the program can simulate the unstable shear crack propagation and failure successfully.

**Fig.33b** shows the good coincidence of analytical and experimental results on the nominal shear strength and the size effect. This agreement ascertained the validity of proposed cracked concrete model and shows the capability of the program **WCOMR** to predict the size effect on shear strength for engineering purpose.

### (4) Mesh sensitivity study

As already stated in section 3(1), the concrete model in RC zone is independent of the size of the control volume of concrete. The concrete model in plain concrete zone is adjusted according to the

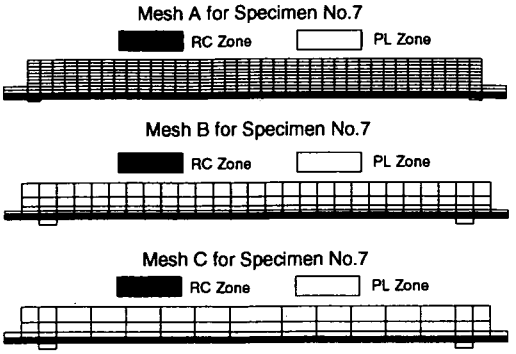


**Fig.34a** Three kinds of mesh for mesh sensitivity study.

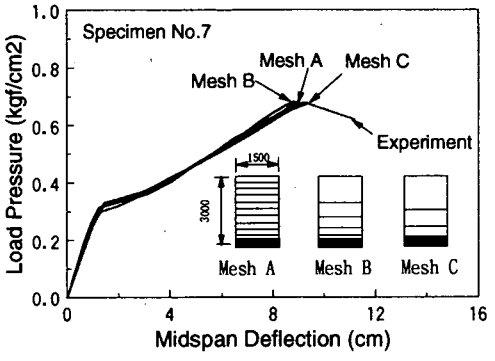


**Fig.34b** Cmputational results for mesh sensitivity study.

fracture energy balance in terms of the element size in computation. In order to examine the mesh sensitivity of finite element analysis, three different meshes are used for computing the Specimen No.7 in the size effect experimental series previously discussed. From Mesh A, B to C, the elements adopted are becoming larger (**Fig.34a**), and the analytical results are shown in **Fig.34b**. It can be seen that the effect of mesh size is negligible and the computed shear behavior is successfully common. So, the proposed model offers the stable convergence of the shear capacity even when we further refine element meshes in analysis.

## 5. VERIFICATION OF THE SIZE EFFECT MECHANISM ON SHEAR STRENGTH OF RC BEAMS

As discussed above, the major mechanical sources of size effect on shear strength of RC members without shear reinforcement are assumed to be 1) tensile stress-strain softening described by the fracture energy law; 2) bond effect of reinforcing bars; and 3) shear strain softening of concrete along cracks. Here, some computation will be reported for verification of these assumptions and the effects of

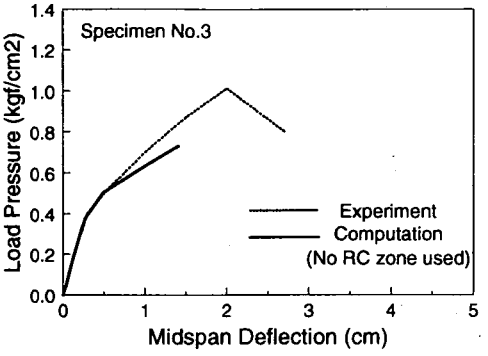


**Fig.35a** Computation for specimen No.3(No RC zone used).

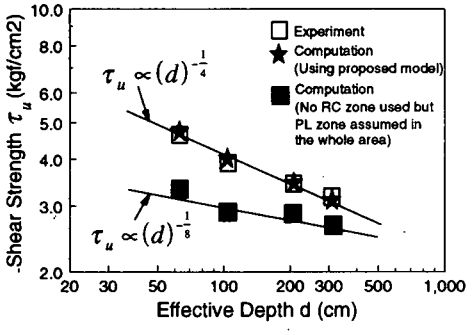


**Fig.35b** RC zone effect on size effect computation.

these sources will be discussed based on systematically arranged sensitivity study. The size effect tests with the maximum beam depth of 300cm is used here as the target. As the specimens No.1 and No.2 do not fail in shear mode in the test, only specimen No.3,5,6 and 7 will be analyzed.

### (1) The effect of bond

It has been discussed by many researchers that the tensile stress-strain softening based on the fracture energy may explain the size effect of plain concrete. But, how the bond can affect the size effect of RC is still a question. It is needed to study what kind of size effect would be derived if the bond effect or the tension-stiffening of the concrete in RC zone were ignored. **Fig.35a** shows the result of specimen No.3 when no RC zone is considered in computation but the plain concrete model is applied to the whole volume of the structure. It can be seen that the specimen would fail earlier than the test, and the stiffness is a little smaller. The computation for other three specimen is similar to specimen No.3. The ignorance of tension-stiffening rooted in bond mechanism is the cause of smaller stiffness and the associated shear softening brings about the premature shear failure.

Even though all calculated strengths for these four specimens are lower than the experimental ones, there is still a size effect tendency as **Fig.35b**.

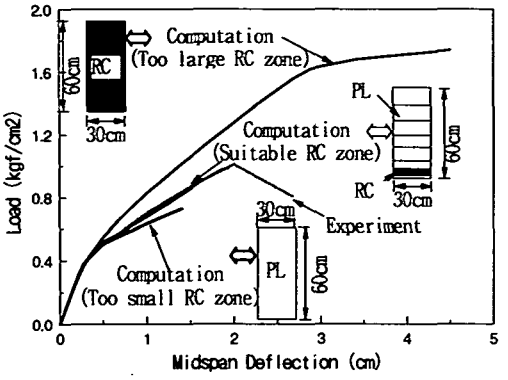


**Fig.36** Effect of RC zone size on computation of shear capacity.

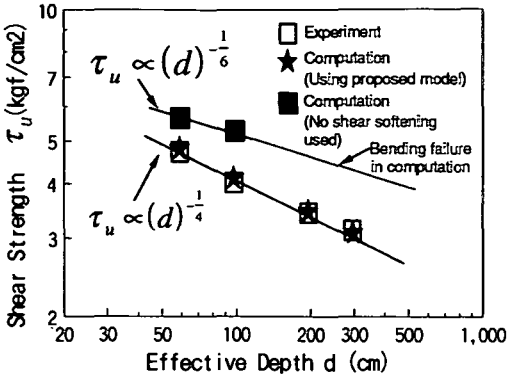


**Fig.38** Shear softening effect on size effect computation.

The size effect tendency can be shown closely as straight lines in logarithmic coordinates. It shows that the computation which adopts the proposed model and the zoning method gives the size effect close to the test result and the size effect sensitivity is sharper than the computation without considering the RC zone. If we do not take into account the bond effect in RC zone, the size effect and shear capacity become less (**Fig.35b**).

The zoning method is also very important as different size of RC zone will give totally different result when simulating the experiment. The stiffness after cracking is obviously higher if larger RC zone is defined in the computation (**Fig.36**). As the concrete in RC zone carries some load even after cracking, the yielding point is overestimated when the RC zone is decided larger than the reality.

**(2) The effect of shear softening**

Another factor to be investigated is the effect of shear softening. In this section, the computation was done without shear softening. It means that the original contact density model[18] without shear progressive softening was applied, and the Bujadham model was not used. In order to separate the shear softening effect on shear behavior of RC beams from other factors, all the other conditions, the tensile softening and bond effect in RC zone were kept the same as the proposed model.

The computational results of specimen No.3,5,6 and 7 are shown in **Fig.37**. In the computation, the beam No.3 failed with shear mode, but much higher than the real case. Beam No.5 failed near the yielding point of main reinforcement, but still in shear mode and shear capacity also became higher. Beam No.6 and 7 failed in bending mode.

The first point we can get from these results is that the shear softening and shear stiffening affect the shear capacity alone. But it does not change the stiffness behavior and the yielding load of the RC member.

As pointed above, the larger member fails earlier as a fact of strain-softening based on the fracture energy law. This is also true for the shear failure. When the shear softening model for plain concrete is changed into stiffening model, the larger beam gets larger capacity and becomes more difficult to fail. At the same time, the size effect tendency becomes lighter. This can be found in **Fig.38**. Approximately 20-25% of the shear capacity of beams is influenced by the shear softening feature of plain concrete crack band.

**(3) The effect of shear transfer after cracking**

In this section, the effect of shear transfer after cracking is discussed. In the whole section of the beam, either RC zone or PL zone, if the shear transfer capability would be lost immediately after cracking, how the shear capacity and the size effect tendency be affected is the point of discussion. In the computation, all the other factors, i.e, the tensile softening and bond effect in RC zone, were kept the same as the proposed model.

The computed load-deflection relationships for the specimens No.3 and No.7 are shown in **Fig.39**. It can be seen that the computed shear capacity decreased a little if the shear transfer was neglected. The results of the case when only the shear transfer of plain concrete zone was neglected are also shown in this figure. The difference is not so large because the RC zone is comparatively small in these beams.

The shear transfer on size effect tendency is shown in **Fig.40.** We can see that when the shear transfer of the whole section is not considered in the computation, the size effect tendency becomes a little less. In the case of larger RC zone, the shear transfer will affect the shear capacity much. Here is an example of a beam whose entire volume is assumed as RC zone. **Fig.41** shows the layout of the experiment.

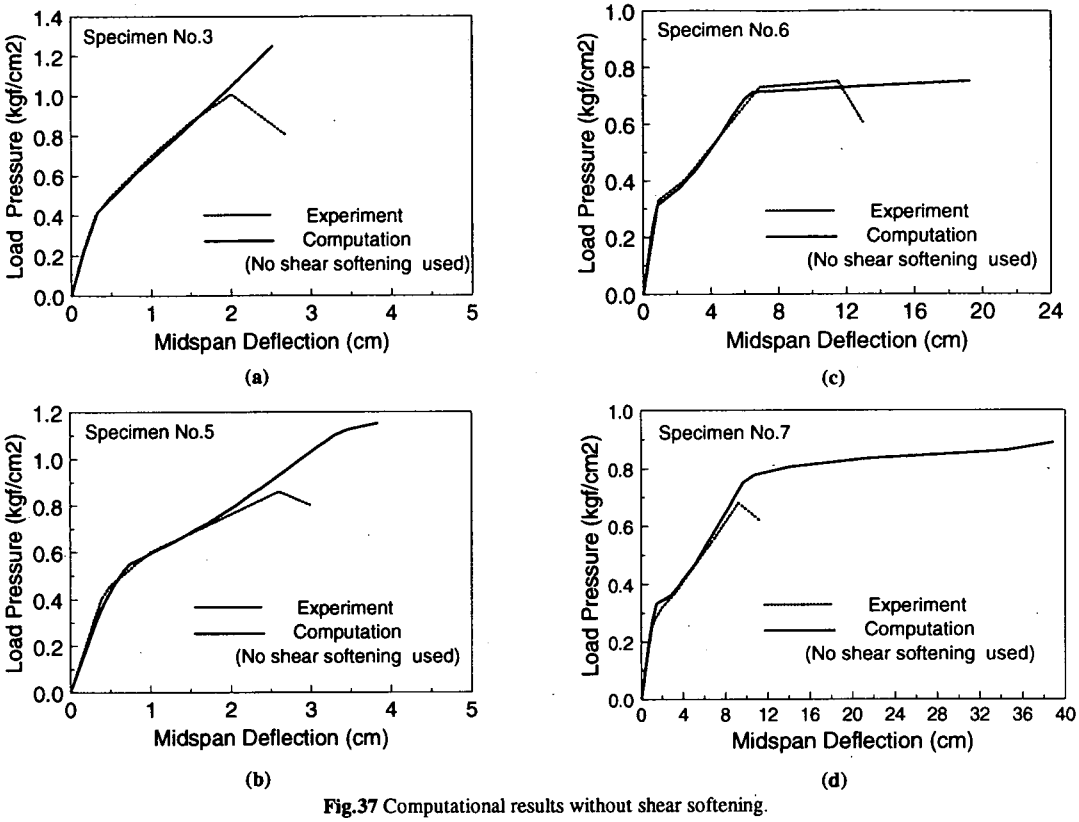


**Fig.37** Computational results without shear softening.

The computational results are shown in **Fig.42**, comparing with the experimental results. In experiment, the beam finally failed in shear accompanying the yield of web reinforcement. In fact, the estimated bending failure load is about 300 tonf beyond the actual capacity. Form the comparison we can see that in the case of large RC zone, the ignorance of shear transfer after cracking brings about the shear capacity much lower than the reality.

**(4) JSCE code equation on shear**

As shown above, the proposed model may predict the size effect in shear of RC beams. The predicted size effect is proportional to $d^{-1/4}$, which is similar to the JSCE shear capacity equation[31] as,

$$V_c = 0.9\left[\left(100\rho\ f'_c\right)^{1/3}(d/100)^{-1/4}\right]\cdot b_w d \quad (9)$$

where, $V_c$ : the shear capacity (kgf), $b_w$ : the member width, $d$ : effective depth, $\rho$ : the reinforcement ratio, $f_c'$ :compressive strength (kgf/cm$^2$).

In order to verify the proposed model on shear strength prediction, computation was carried out for a beam with depth 95cm (**Fig.43**) and the shear strength varying with different reinforcement ratio and concrete strength. The results are plotted in **Fig.43** and **Fig.44**. Here, the tensile strength used in **Eq.(2)** is estimated by the conversion equation[16] from the compressive strength of concrete as shown in **Fig.44**, and the tensile fracture energy is defined by the estimation included in **Fig.18**. The predicted shear strength is proportional to $\rho^{1/3}$ and $f_c'^{1/3}$. So, the computation has fair agreement with the JSCE code equation.

**(5) The effect of axial stress on shear strength**

It is found that the axial force affects the shear strength of RC beams. The compressive axial force increases the shear capacity of the beam and the tension force has contrary effect. The effect of axial force can be simulated by FEM computation. The axial stresses acting on the beam are from 15kgf/cm$^2$ to -15kgf/cm$^2$. The other factors of the beam are kept constant in the computation.

The computation results are plotted in **Fig.45.** It can been seen the shear strength of this beam changes with the varying axial mean stress. The shear strength is linearly changed with the variation of axial tension or compression stress, and the effect of tension stress is almost 2 times as the effect of compression stress.

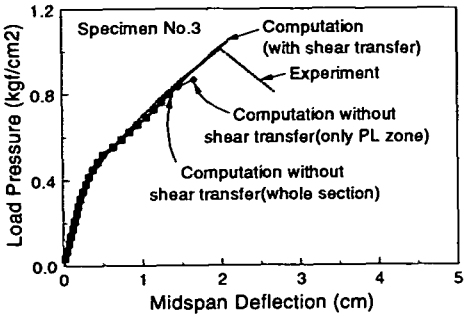


(a)

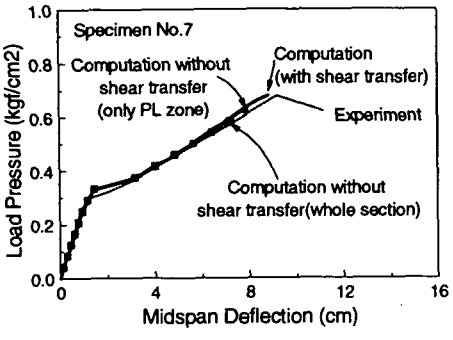


(b)

**Fig.39** Shear stiffness and strength without shear transfer.

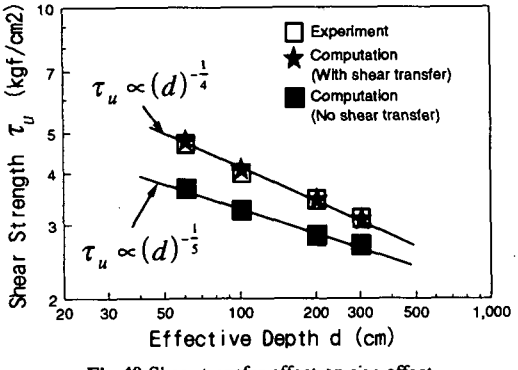


**Fig.40** Shear transfer effect on size effect.

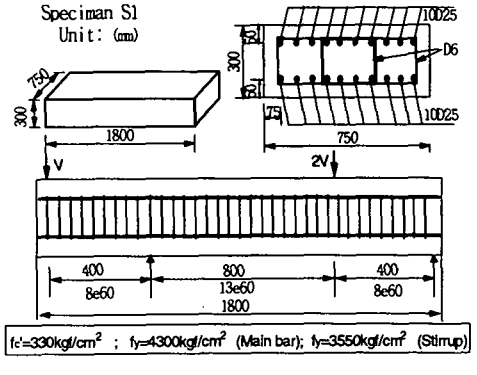


**Fig.41** Layout of the specimen used for checking shear transfer effect.

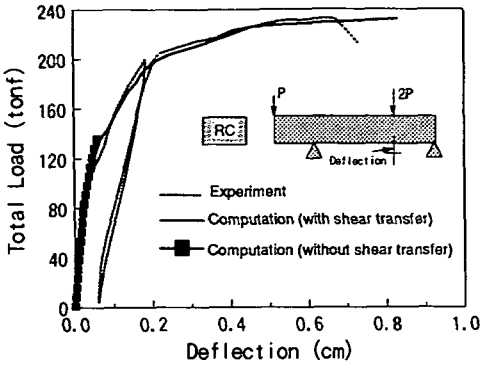


**Fig.42** Shear transfer effect on shear strength prediction.

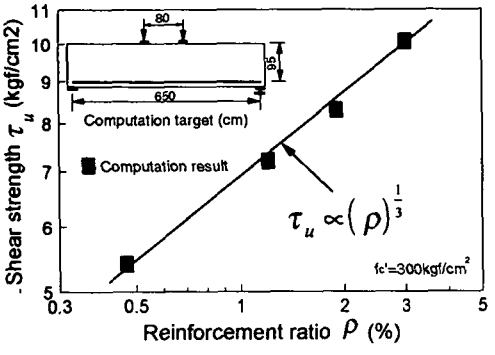


**Fig.43** Effect of reinforcement ration on shear strength.

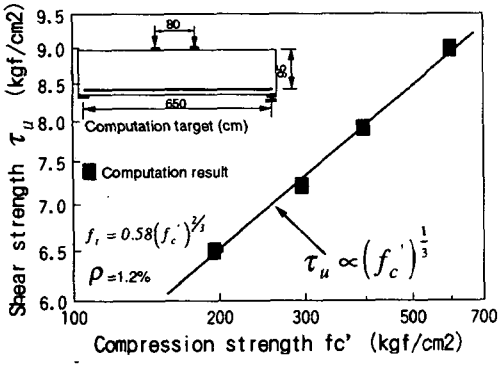


**Fig.44** Effect of concrete strength on shear strength.

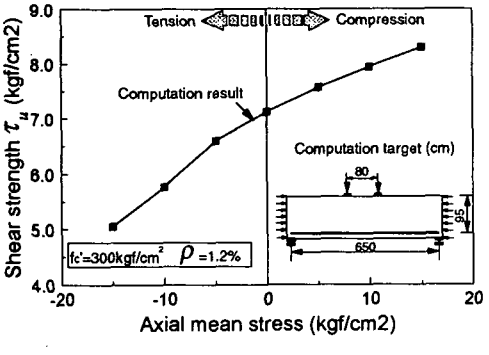


**Fig.45** Effect of axial stress on shear strength.

## 6. CONCLUSIONS

The mechanism of size effect on shear strength was discussed in this study. Tension and shear softening of cracked concrete based on the fracture energy and bond effect of steel and concrete are clearly and quantitatively regarded as the major sources which control the shear behavior and size effect. The computation shows that any of these factors cannot be ignored in simulating the size effect on shear strength of RC beams without shear reinforcement.

The model which combines the nonlinearity of cracked concrete in RC zone and plain concrete zone was proposed and adopted to FEM nonlinear analysis. The RC zoning method was discussed to decide correctly the size of RC zone in which cracks are dispersed owing to the stable stress transfer through bond mechanism. The computations for bending and shear tests show that the proposed model can simulate the shear. The FEM program using the proposed model was used to simulate the size effect of RC beams without shear reinforcement. The computational and experimental results were found to coincide closely. It has been verified that the proposed model can be used for predicting shear behavior and size effect in engineering purpose.

In this study, different sensitivity of apparent size effects was computed in accordance with the shape of beams, aggregate sizes, assumed material models, etc. In the next step, more clear understanding of the size effect sensitivity should be quantitatively sought.

Finally, it must be noted that the discussions herein are limited within the shear failure prior to yielding of longitudinal reinforcement. The post-yield shear failure and associated ductility will be discussed in future study.

**ACKNOWLEDGMENT**: This study was conducted with financial support Grant-in-Aid for Scientific Research No.07455180 from Ministry of Education, Science and Culture.

### REFERENCES

1) Kani,G.N.J. : How safe are our large reinforced concrete beams?, *Journal of ACI*, No.64-12, pp.128-141, 1967.
2) Taylor,H.P.J. : Shear strength of large beams, *Journal of Structural Division*, Proc. of ASCE, pp2473-2490, 1972.
3) Swamy, R.N. and Qureshi, S.A. : Strength, cracking and deforamtion similitude in reinforced T-beams under bending and shear, *Journal of ACI*, pp.187-195, 1971.
4) Iguro, M. and Shioya, T. : Experimental studies on shear strength of large reinforced concrete beams under uniformly distributed load, *Concrete Library of JSCE*, No.5, pp137-154, 1985.
5) Okamura, H. and Maekawa, K. : Reinforced concrete design and size effect in structural nonlinearity, invited, *Proceeding of JCI International Workshop*, Sendai, Japan, pp.1-20,1993.
6) Shirai, N. : JCI round robin analysis in size effect in concrete structures, *Proceeding of JCI International Workshop*, Sendai, Japan, pp.247-270, 1993.
7) JCI : *Report on the research and application of fracture mechanics*, 1993.
8) Mihashi, H. : Chapter 4.3, A stochastic theory for fracture of concrete, *Fracture mechanics of concrete*, F.H. Wittman, ed., Elsevier, New York, N.Y., pp301-340, 1983.
9) Bazant, Z.P. and Xi, Y. : Statistical size effect in quasibrittle structures, *J. Engrg Mech., ASCE*,117(11), pp2609-2640, 1991.
10) Shioya, T. and Okada, T. : The effect of the maximum aggregate size on shear strength of reinforced concrete beams, *JCI, 7th Annual Convention*, pp.521-524, 1985.
11) Bazant, Z.P., Ozbolt, J. and Eligehausen, R. : Fracture size effect: review of evidence for concrete structures, *Journal of Structural Eng.*, ASCE, Vol.120, No.8, pp2377-2398, 1992.
12) Bazant, Z.P. and Oh, B.H. : Crack band theory for fracture of concrete, *Material and Structures*, (RILEM, Prais), Vol.16, pp155-157, 1983.
13) Bazant, Z.P. : Size effect in blunt fracture: concrete, rock, metal, *Journal of Engineering Mech.*,Vol110,No.4,pp518-535, 1983.
14) Collins, M. P. and Mitchell, D. : *Prestressed concrete structures*, PRENTICE HALL, Englewood Cliffs, New Jersey 07632, 1991.
15) Goto, Y. : Cracks formed in concrete around deformed tension bars, *Journal of ACI*, Vol.68,No.4, pp.224-251, 1971.
16) Okamura, H. and Maekawa, K. : *Nonlinear Analysis and Constitutive Models of Reinforced Concrete*, Gihodo-Shuppan, Tokyo, Japan, 1991.
17) Okamura, H., Maekawa, K. and Sivasubramaniyam, S. : Verification of modeling for reinforced concrete finite element, *Finite element analysis in reinforced concrete structures*, ASCE, pp528-543, 1985.
18) Li, B., Maekawa, K. and Okamura, H. : Contact density model for stress tranfer across cracks in concrete, *Journal of the Faculty of Engineering, University of Tokyo (B)*, Vol.40, No.1, pp.9-52, 1989.
19) Tepfers,R. : A theory of bond applied to overlapped tensile reinforcement splices for deformed bars, *Publication 73:2,Division of Concrete Structures, Chalmers University of Technology*, Goteborg, Sweden, 1973.
20) Jinno, Y., Fujii, S. and Morita, S. : Bar size effect on bond characteristics with splitting of surrounding concrete, *Summaries of technical papers of annual meeting*, AIJ, pp747-748, 1986.
21) Morita, S. : Material modeling for finite element analysis of reinforced concrete-recent development in Japan, *Report of 2nd Japan-U.S. seminar on finite element analysis of reinforced concrete*, New York, Publication by JCI, pp107-124, 1991.
22) Zareen, N. and Niwa, J. : Nonlinear finite element analysis for prediction of size effect of concrete beams based on fracture mechanics, *JCI International Workshop on Size Effect in Concrete Structures*, Sendai, Japan, 1993.
23) Shima, H. : Micro and macro models for bond behavior in reinforced concrete, *Jr. of the Faculty of Eng., the Univ. of Tokyo*, 1986.
24) Shin, Hyun Mock : *Finite Element Analysis of Reinforced Concrete Members Subjected to Reversed Cyclic In-Plane Loading*, Doctor Dissertation, Tokyo University, 1988.
25) Collins, M.P. : The shear strength of reinforced concrete structures, invited, *JCI annual convention*, 1995.

26) Walraven, J. C. : Size effect: their nature and their recognition in building codes, *Proceeding of JCI International Workshop*, Sendai, Japan, pp.295-314, 1993.
27) Bujadham, B. and Maekawa, K. : Qualitative studies on mechanisms of stress transfer across cracks in concrete, *Proc.of JSCE*, No.451/V-17, pp265-275, 1992.
28) Bujadham, B. and Maekawa, K. : The universal model for stress transter across cracks in concrete, *Proc.of JSCE*, No.451/V-17, pp277-287, 1992.
29) Bujadham, B., Mishima, T. and Maekawa, K. : Verification of the universal stress transfer model, *Proc.of JSCE*, No.451/V-17, pp289-300, 1992.
30) Maekawa, K. and Hasegawa, T. : The state-of-the-art on constitutive laws of concrete, *Concrete Journal*, Vol.32, No.5, pp.13-22, 1994.
31) JSCE, *Standard specification for design and construction of concrete structure, part I(Design)*, First edition, Tokyo, 1986.
32) Rots, J.G. and Nauta, P. : Variable reduction factor for the shear stiffness of cracked concrete, Pre. BI-84-33, Institute TNO for Building Material and Structure, Delft, 1984.
33) Leonhardt, F. and Walther, R. : Beitrage zur Behandlung der Schubprobleme im Stahlbetonbau, 4. fortsetzung des Kapitals II : Versuchsberichte, Beton und Stahlbetonbau, 1962.
34) Maekawa, K., Niwa, J. and Okamura, H. : Computer program "CCOM2" for analyzing reinforced concrete, *Proc. of JCI 2nd Colloquium on Shear Analysis of RC Structures*, JCI-C5, Oct. 1983, pp.79-86.
35) Wittmann, F.H., Rokugo, K., Bruhwiler, E., Mihashi, H. and Simonin, P. : Fracture energy and strain softening of concrete as determined by means of compact tension specimens, *Materials and Structures*, Vol.21, No.121, pp.21-32, 1988.
36) Lim, T.B., Li, B. and Maekawa, K. : Mixed-mode strain-softening model for shear fracture band of concrete subjected to in-plane shear and normal compression, *Proc. of Int. Conf. on Computational Plasticity*, Barcelona, June, pp.1431-1444, 1987.

**(Received April 5, 1996)**

## RCはりのせん断強度に現れる寸法効果の数値シミュレーション

Xuehui AN・前川宏一・岡村　甫

本研究は，主鉄筋降伏以前に発生するRCはりのせん断破壊と強度に現れる寸法効果について有限要素解析による解析を行い，使用した構成モデルの妥当性の検証と機構に関する検討を報告するものである．鉄筋コンクリート領域を，鉄筋との付着作用によってひび割れ以後も十分な引張応力の伝達が期待できる領域と，急激な引っ張り軟化を呈する無筋領域とに分割し，個々に引張およびせん断伝達に硬化及び軟化モデルを適用することを提案している．釣り合い解を探索する繰り返し計算中に進展するひび割れ領域の観察から，せん断破壊モードを数値的に判定する方法を提示するとともに，はりのせん断破壊に現れる寸法効果を解析的に示した．